12. J. R. M. Innes *et al., J. Natl. Cancer Inst.* **42**, 1101 (1969).
13. "Bioassay of sulfallate for possible carcinogenicity," *Natl. Cancer Inst. Carcinogenesis Tech. Rep. Ser. 115, DHEW Publ. (NIH) 78-1370* (1978).
14. B. N. Ames, J. McCann, E. Yamasaki, *Mutat. Res.* **31**, 347 (1975).
15. Supported in part by NIH grant 5 P01 ES00049. For advice and assistance we thank B. N. Ames of the Department of Biochemistry (University of California, Berkeley) and Y. -L. Chen and R. L. Holmstead of the Pesticide Chemistry and Toxicology Laboratory.
* Permanent address: Institute of Pesticide Research, Federal Biological Research Center, D-1000 Berlin 33, Federal Republic of Germany.
† Permanent address: Department of Food Science, Cook College, Rutgers University, New Brunswick, N.J. 08903.

12 February 1979; revised 20 April 1979

Visual Resolution and Receptive Field Size: Examination of Two Kinds of Cat Retinal Ganglion Cell

Abstract. *Intraocular recordings from brisk-sustained and brisk-transient ganglion cells in the cat's retina revealed a systematic increase in center size and decrease in spatial cut-off frequency with increasing distance from the area centralis. At any one eccentricity sizes of the centers of sustained and transient cells did not overlap, and the variation in cut-off frequency for each class was constrained to about one-half octave.*

Spatial inhomogeneity within the visual system is reflected in the variation in spatial resolution across the visual field. Thus visual acuity is highest in the fovea and declines progressively as stimulation is moved towards the periphery (*1*). This reduction in spatial resolution is attributed to several factors associated with increasing eccentricity, among them a decline in receptor and ganglion cell density (*2, 3*), a decrease in cortical magnification (*4*), and an increase in receptive field size (*5-7*). We performed experiments to show how both spatial resolution and receptive field size of selected classes of cat retinal ganglion cells vary as a function of eccentricity, and in addition to determine the local variability of these two measures.

The retinal ganglion-cell mosaic is made up of many types of ganglion cells (*6, 7*), which likely subserve different visual functions. It is therefore not sufficient to describe general trends in receptive field properties of ganglion cells taken as a whole; rather, we need knowledge of receptive field properties within a single class as a function of retinal position. This kind of information is most readily obtained through the use of intraocular recording techniques that allow the position of the microelectrode to be varied systematically and accurately. Moreover, it is essential to collect data from as many units as possible within a single retina, for pooling data from several experiments inflates the observed variability.

This report deals only with on-center units with brisk properties (*7*). In all, 180 ganglion cells (138 brisk-sustained units and 42 brisk-transient units) were studied in four cats. In all but seven of these units, we measured, as a function of retinal eccentricity (i) the size of the receptive field center (bar stimuli) and (ii) the spatial cut-off frequency (spatial frequency beyond which there is no significant modulated response) (high-contrast, square-wave gratings). We have specifically avoided examining the unmodulated response observed in brisk-transient units by using fine gratings (*6*).

Experimental methods are essentially the same as those used by Cleland and Levick (*7*). Anesthesia was induced in adult cats by ventilation of 3 to 4 percent halothane in a 2:1 gas mixture of nitrous oxide and carbogen and was maintained during preparatory surgery with 1 to 1.5 percent halothane. To reduce eye movements, the left vagosympathetic trunk was cut and the animal paralyzed by continuous intravenous infusion of an isotonic solution (4 ml/hour) of Flaxedil (5 mg per kilogram of body weight per hour), *d*-tubocurarine (0.4 mg/kg-hour), and glucose. End-tidal P_{CO_2} was monitored and kept at 4 percent by adjusting the stroke volume of the respirator. Bipolar stimulating electrodes (platinum iridium wire in glass) were stereotaxically placed in the left and right optic tracts. The left eye was secured to a micromanipulator by suturing a flap of conjunctiva to a metal ring encircling the globe. The sclera was punctured with a sealed hypodermic needle which allowed the insertion of a tungsten microelectrode (*8*) into the posterior chamber and the precise positioning of the micro-

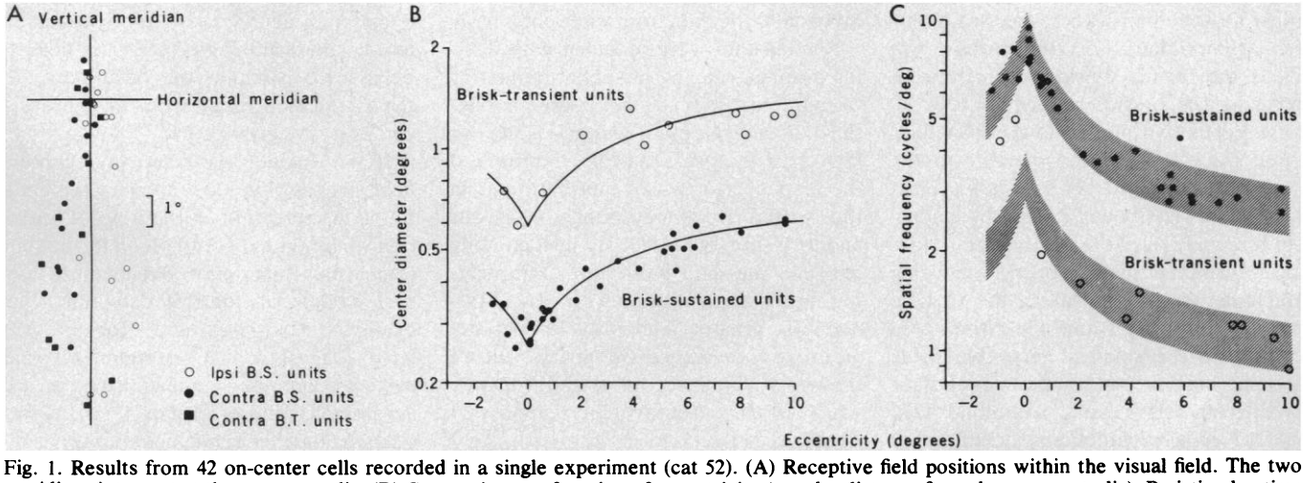

Fig. 1. Results from 42 on-center cells recorded in a single experiment (cat 52). (A) Receptive field positions within the visual field. The two meridians intersect at the area centralis. (B) Center size as a function of eccentricity (angular distance from the area centralis). Peristimulus-time histograms describing the results for a bar (luminance, 25 cd/m², background, 3 cd/m²) moving slowly across the receptive field. Center size was taken as the width of the peak of the histogram at the level of the maintained firing. (C) Spatial cut-off frequency as a function of eccentricity. The shaded area represents a one-quarter octave above and below a hyperbolic curve (reflected) fitted to the sustained units. This area is moved vertically to fit the transient units. Cut-off frequency was estimated from peristimulus-time histograms describing the results of square-wave gratings (mean luminance, 150 cd/m²; contrast, 0.84) moving across the receptive field. Drift frequency, 4 cycles per second.

0036-8075/79/0907-1015$00.50/0

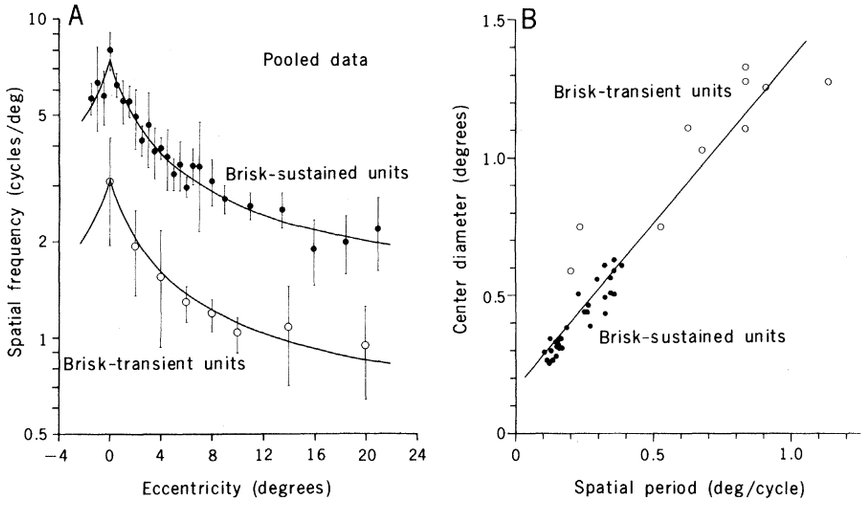

Fig. 2. (A) Spatial cut-off frequency as a function of eccentricity (pooled data). Bin widths for the sustained units are 0.5° at smaller eccentricities increasing to 3° at larger eccentricities. Transient units have larger bin widths consistent with sample size. Vertical bars represent 1 standard deviation. (B) Relationship between center diameter and spatial period (1 divided by cut-off frequency) for data in Fig. 1.

electrode on the retina. Neosynephrine and atropine were used to retract the nictitating membrane and dilate the pupil. A contact lens of zero power was fitted to the cornea to keep it moist. During the period of data collection, halothane was removed from the gas mixture.

The eye was made to focus upon a tangent screen at a distance of 114 cm by placing in front of the eye a spectacle lens chosen to optimize the spatial resolution of recorded brisk-sustained units. A 3-mm (diameter) artificial pupil was used to minimize spherical aberration and assure good depth of field. Neural activity was elicited by moving patterns projected onto the screen.

Because of the radial asymmetry of ganglion cell density as a function of eccentricity (*3*), receptive field properties must be specified with respect to a particular meridian. For this purpose we chose the vertical meridian, which is defined as the border between brisk-sustained cells that project to the ipsilateral optic tract and those projecting to the contralateral optic tract (*9*). Such projections were readily determined by electrical stimulation of the optic tracts. Having determined this border, the recording electrode was moved along the vertical meridian until we found the retinal area containing the smallest receptive fields and the longest antidromic latencies for brisk-sustained cells. This retinal area was taken as a functional definition of the area centralis.

Figure 1A shows the visual field position of the receptive fields of 42 brisk ganglion cells recorded in a single retina. The receptive field center diameters were determined from histograms collected as a light bar (0.1° wide, 10° long) moved slowly (0.5° per second, 5° per second, or both) backward and forward across the receptive field. We chose as our measure the width of the response at the level of the maintained discharge averaged over the two directions of movement. In Fig. 1B, center diameter is plotted as a function of distance from the middle of the area centralis. Center sizes are smallest in the area centralis and monotonically increase with eccentricity; at each retinal position diameters of sustained and transient units do not overlap. Data from sustained units have been fitted with a segment of a hyperbolic curve (*10*) that is reflected about a vertical line passing through the area centralis. Vertical translation of the curve shows that it also provides an adequate fit to the data from transient units.

Similar data were obtained with drifting gratings ranging in spatial frequency from 0.5 to 8.0 cycles per degree in one-third octave steps. For each unit, we measured the peak-to-peak amplitude of the response to two or more gratings in the spatial frequency range near our auditory threshold (*11*). By interpolating between the data points (or extrapolating, in the case of units with cut-off frequencies greater than 8 cycles per degree) we determined the spatial cut-off frequency, defined as that frequency which produced an average response of 25 spikes per second.

Data pooled from four cats are shown in Fig. 2A, with each point representing the average of at least three observations. The data for the brisk-sustained units are fitted by a hyperbolic curve with the data points showing very little deviation from the curve. The same curve moved vertically also provides a good fit to the data from brisk-transient units. Thus the ratio of brisk-transient to brisk-sustained resolution is the same at all eccentricities. For each class, resolution is highest in the center of the area centralis and has fallen by a factor of 2 at about 4° of eccentricity.

Pooled data, however, are largely limited to a demonstration of central tendency; in Fig. 1C, the variation in cut-off frequency with distance from the area centralis is shown for a single animal. Again, the data do not overlap. Cut-off frequency falls more rapidly with eccentricity near the area centralis and less in the periphery. To provide an estimate of the distribution in cut-off frequencies at each eccentricity, we have again fitted a hyperbolic function. Typically, 90 percent of our data points fall within a one-half octave variation in frequency. Occasionally, brisk-transient units near the area centralis had cut-off frequencies that seem unusually high (Fig. 1C), but the sizes of their receptive field centers appeared normal and were within the expected range.

To show consistency of our two measures, center size versus the spatial period of the cut-off frequency for each of 40 ganglion cells is plotted in Fig. 2B (r = .96). Both sustained and transient cells cluster around a single regression line (slope, 1.20; intercept, 0.16). For the other three cats, the regression slopes were 1.38, 1.79, and 2.17, and the intercepts 0.08, 0.03, and 0.02, respectively.

In the center of the area centralis, brisk-sustained units have cut-off frequencies as high as 9.5 cycles per degree (for example, Fig. 1C). Although units with cut-off frequencies greater than 8 cycles per degree were rarely encountered, our results agree with the highest behavioral estimates of visual acuity in the cat, which range from about 6 to 9 cycles per degree (*12*).

If the variation we see in receptive field sizes within local areas of the cat's retina is indicative of the kind of variation we might expect to see in the human retina, these data may be relevant to current models of contrast detection. For example, Campbell and Robson (*13*) have suggested that the human visual system contains channels which are sensitive to different bands of spatial frequency. Further refinements to this suggestion point to the possibility that multiple channels may exist at all eccentricities, although interpretations differ (*14, 15*). Generally, the psychophysical data are best fitted by one of two models. According to the nomenclature of Graham

et al. (*15*), they are space-variant single- and multiple-channel models. Both models allow for increases in receptive field sizes with increasing eccentricity, but they differ in their allotment of the number of receptive field sizes at any one particular eccentricity; the single-channel model allows for one and the multiple-channel model for several sizes.

Our data show unequivocally that at any one area of retina, brisk ganglion cells of the same kind are closely matched in their spatial properties. It is only when we consider cells of different classes, that we see a range in sizes of neighboring concentric receptive fields with the upper and lower bounds being determined by brisk-transient and brisk-sustained units, respectively (*7*).

It seems reasonable to suggest that visual stimuli used in detection tasks may preferentially stimulate one kind of ganglion cell rather than another and therefore lead to unique thresholds. For example, Wilson (*16*) has shown in humans that by presenting line stimuli with temporal modulations which maximize either sustained or transient responses, two neural mechanisms can be detected at each retinal position. The mechanism characterized by the sustained response property responds to higher spatial frequencies than does the mechanism characterized by transient response properties, a finding in agreement with our neurophysiological findings in the cat.

B. G. CLELAND
T. H. HARDING
U. TULUNAY-KEESEY

Department of Physiology,
Australian National University,
Canberra City, A.C.T. 2601

References and Notes

1. T. H. Wertheim, *Z. Psychol. Physiol. Sinnesorg.* **7**, 172 (1894); F. W. Weymouth, D. C. Hines, L. H. Acres, J. E. Raaf, M. C. Wheeler, *Am J. Ophthalmol.* **11**, 947 (1928); E. Ludvigh, *ibid.* **24**, 303 (1941); H. G. Randall, D. J. Brown, L. L. Sloan, *Arch. Ophthalmol.* **75**, 500 (1966); D. G. Green, *J. Physiol. (London)* **207**, 351 (1970); S. M. Anstis, *Vision Res.* **14**, 589 (1974); M. A. Berkley, F. Kitterle, D. W. Watkins, *ibid.* **15**, 239 (1975).
2. G. Österberg *Acta Ophthalmol. (Copenhagen) Suppl.* **6** (1935); V. Vilter, *C. R. Seances Soc. Biol. Paris* **143**, 830 (1949); J. M. Van Buren, *The Retinal Ganglion Cell Layer* (Thomas, Springfield, Ill., 1963); O. Oppel, in *Eye Structure*, S. W. Rohen, Ed. (Schattauer, Stuttgart, 1965), vol. 2, p. 97.
3. J. Stone, *J. Comp. Neurol.* **124**, 337 (1965); H. Wässle, W. R. Levick, B. G. Cleland, *ibid.* **159**, 419 (1975); A. Hughes, *ibid.* **163**, 107 (1975).
4. P. M. Daniel and D. Whitteridge, *J. Physiol. (London)* **159**, 203 (1961); E. T. Rolls and A. Cowey, *Exp. Brain Res.* **10**, 298 (1970); A. Cowey and E. T. Rolls, *ibid.* **21**, 447 (1974).
5. T. N. Wiesel, *J. Physiol. (London)* **153**, 583 (1960); D. H. Hubel and T. N. Wiesel, *ibid.* **154**, 572 (1960); H. Ikeda and M. J. Wright, *Vision Res.* **12**, 1465 (1972); B. Fischer, *ibid.* **13**, 2113 (1973); J. R. Wilson and S. M. Sherman, *J. Neurophysiol.* **39**, 512 (1976).
6. C. Enroth-Cugell and J. G. Robson, *J. Physiol. (London)* **187**, 517 (1966); J. Stone and Y. Fukuda, *J. Neurophysiol.* **37**, 722 (1974).
7. B. G. Cleland and W. R. Levick, *J. Physiol. (London)* **240**, 421 (1974).
8. W. R. Levick, *Med. Electron. Biol. Eng.* **10**, 510 (1972).
9. D. L. Kirk, W. R. Levick, B. G. Cleland, H. Wässle, *Vision Res.* **16**, 225 (1976).
10. A hyperbolic function of the form $y - y_0 = c/(|x| - x_0)$, although somewhat arbitrarily selected, describes both the decline in cut-off frequency and the increase in the size of the receptive field center with increasing eccentricity.
11. As the bars of a coarse grating are moved across the receptive field of a ganglion cell, a variation in the response can be heard in the spike discharge as amplified through a loudspeaker. As the grating frequency is increased, but with the velocity adjusted to give a constant temporal modulation, the amplitude of the response grows weaker until an auditory threshold is reached. We found this threshold when averaged responses showed a peak-to-peak amplitude of about 25 spikes per second.
12. K. U. Smith, *J. Gen. Psychol.* **49**, 297 (1936); R. Blake, S. J. Cool, M. L. J. Crawford, *Vision Res.* **14**, 1211 (1974); S. G. Jacobson, K. B. J. Franklin, W. I. McDonald, *ibid.* **16**, 1141 (1976); D. E. Mitchell, F. Giffin, B. Timney, *Perception* **6**, 181 (1977).
13. F. W. Campbell and J. G. Robson, *J. Physiol. (London)* **197**, 551 (1968).
14. M. B. Sachs, J. Nachmias, J. G. Robson, *J. Opt. Soc. Am.* **61**, 1176 (1971); N. Graham and J. Nachmias, *Vision Res.* **11**, 251 (1971); A. J. van Dorn, J. J. Koenderink, M. A. Bouman, *Kybernetik* **10**, 223 (1972); P. E. King-Smith and J. J. Kulikowski, *J. Physiol. (London)* **247**, 237 (1975); C. F. Stromeyer and S. Klein, *Vision Res.* **15**, 899 (1975); M. Hines, *ibid.* **16**, 567 (1976); J. O. Limb and C. B. Rubinstein, *ibid.* **17**, 571 (1977); H. R. Wilson and S. C. Giese, *ibid.* p. 1177.
15. N. Graham, J. G. Robson, J. Nachmias, *Vision Res.* **18**, 815 (1978).
16. H. R. Wilson, *ibid.*, p. 971.
17. We thank B. McLachlan for her valuable technical assistance and appreciate the many contributions of the technical staff of the Physiology Department and members of the Photographic Unit. This work was supported by postdoctoral fellowship (to T.H.) 5 F32 EY05194 and grant EY 00308 (to U.T.-K.) from the National Institutes of Health.

6 March 1979; revised 31 May 1979

The Central Origin of Efferent Pathways in the Carotid Sinus Nerve of the Cat

Abstract. *The application of horseradish peroxidase to the central cut end of the carotid sinus nerve of the cat produced retrograde labeling of neurons in the ipsilateral medulla in the region of the nucleus ambiguus at anterior-posterior coordinates −8 to −10.5. These data coupled with previous electrophysiological observations suggest that the nucleus ambiguus may be the origin of an efferent inhibitory pathway to the carotid body.*

The carotid sinus nerve contains efferent fibers as well as chemoreceptor and baroreceptor afferents (*1*). Activation of the efferent pathway inhibits chemoreceptor firing (*2*). These observations prompted the hypothesis that efferent axons make excitatory synaptic contacts in the carotid body with type 1 cells, which in turn release an inhibitory substance that depresses afferent activity (*3*). It has also been suggested that efferent activity produces in the carotid body vascular changes that indirectly alter chemoreceptor firing (*4, 5*).

The origin of the sinus nerve efferent pathways is uncertain. Initial electron microscopy (*3*) revealed that efferent contacts with type-1 cells degenerate after intracranial section of the glossopharyngeal nerve, which indicates that the efferent fibers originated in the brainstem. However, subsequent investigations could not confirm these findings (*6*).

We used the horseradish peroxidase (HRP) tracing technique to study the origin of efferent fibers in the carotid sinus nerve of the cat. Experiments were conducted on 12 adult cats anesthetized with Dial-urethan. The carotid sinus nerves were unilaterally or bilaterally exposed through a midline incision in the neck. The nerve was sectioned distally near the carotid sinus and placed in a short length (10 mm) of polyethylene tubing, which was filled with HRP solution (Sigma type IV, 25 percent solution in distilled water) and then sealed with petrolatum. The nerve remained in contact with HRP for 4 to 6 hours, after which the solution was removed and the incision closed. After a transport time of 24 to 40 hours, the animal was deeply anesthetized and perfused first with saline and then fixative (1 percent glutaraldehyde and 1 percent paraformaldehyde in 0.05*M* phosphate buffer). The brainstem and petrosal ganglia were removed and stored for 12 to 24 hours in the fixative and then transferred to 5 percent sucrose in phosphate buffer for at least 48 hours before being sectioned. The brainstem was cut on a freezing microtome in 42-μm sections, mounted serially on slides and processed for HRP according to the benzidine method (*7*). In some experiments sections were also counterstained with thionin. Sections were examined with darkfield illumination or with Nomarski optics.

Labeled cells were found in 7 of 12 experiments. They were located in the medulla ipsilateral to the site of HRP application between 10.5 and 8.0 mm posterior to bregma. In individual experiments the cells were distributed over a range from 0.75 to 1.6 mm. The number of labeled cells varied from 3 to 66 ($\bar{X} = 22$, $N = 7$). The cells were oval or spindle-shaped, 10 to 20 μm in diameter and lo-

0036-8075/79/0907-1017$00.50/0